Power Loss and Axial Load Carrying Capacity of Radial Cylindrical Roller Bearings

Simon Söndgen and Wolfgang Predki

This paper is intended to enlarge the application range of radial cylindrical roller bearings by means of a more precise determination of thrust load capacity and more cost-effective design.

Introduction

Cylindrical roller bearings (CRBs) have a wide application range and a significant role in drive engineering. Due to line contact, CRBs have a greater radial load capacity than other rolling bearings of the same size. Their possibility for use in high-speed applications and an advantageous friction behavior are additional benefits (Ref. 1). Several designs, which vary regarding the quantity and arrangement of the lips, exist. The lips allow the application of axial loads in one (supporting bearing) or two directions (locating bearing). When, for example, axial forces are applied, they are transferred from the lip of the inner ring to the roller end faces, and from there to the lip of the outer ring. Alternating axial loads can be supported by a bearing of the NJ (cylindrical roller bearing)-type—in combination with an angle ring HJ (see previous)—or by a bearing of the NUP (see previous)-type with loose lip (Ref. 2).

Despite the fact that combined-loaded CRBs have been in use for more than a century, there had existed no standard for the calculation of the axial load-dependent friction torque and the axial load capacity until now (Ref. 3). While there are indeed equations presented in the relevant literature and bearing catalogues that enable the calculation of the axial load-dependent friction torque, these equations are mostly based on empiric approaches and the results of their use vary significantly.

Lubenow (Ref. 4) conducted extensive measurements on combined-loaded CRBs; Figure 1 shows the results from the equations of Schaeffler (Ref. 5), SKF (Ref. 6), Braendlein (Ref. 7) and the simulation according to Lubenow, as well as the latter's measurement results (Ref. 4). The results shown are valid for a run-in bearing of the NJ 210 type at an operation temperature of 70°C and using lubrication with a mineral oil of the viscosity class ISO VG 220.

The radial load amounts to $F_r = 5$ kN, whereas the axial load $F_a = 4$ kN is chosen. The axial load-dependent friction torque T_2 is illustrated in dependency of the inner ring speed n; Figure 1 shows significant deviations between the different determined axial load-dependent friction torques.

Particularly at low speeds, not only do the results from the equations of the bearing manufacturers and of Braendlein (Ref. 7) vary from the measurement results, but also from Lubenow's simulation results (Ref. 4).

The friction torque of thrust-loaded radial cylindrical roller bearings is an important parameter for the determination of the axial load-carrying capacity at medium to high speeds; the permissible thrust load can be determined by means of a heat balance (Ref. 4). At low speeds, the frictional losses decrease and therefore the theoretically permissible thrust load strongly increases. The bearing manufacturers therefore additionally impose a limiting ratio of axial-to-radial load, and a limit-

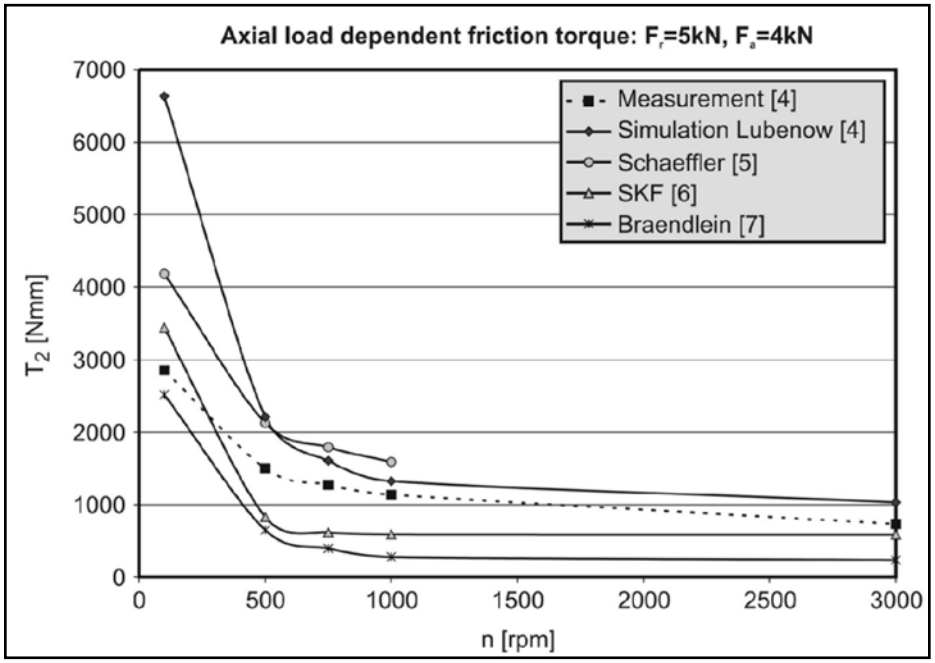

Figure 1 **Axial load-dependent friction torque T_2 according to different calculation methods and measurement results.**

Table 1 Examined bearings and lubricants			
Bore reference number	06	10	16
Bore diameter	$d = 30$ mm	$d = 50$ mm	$d = 80$ mm
Variant	NJ2206 E.TVP2	NJ2210 E.TVP2	NJ2216 E.TVP2
	N2306 E.TVP2	NJ2310 E.TVP2	
	NUP2206 E.TVP2	NUP2210 E.TVP2	
	NJ2206 E.TVP2 + HJ206	NJ2210 E.TVP2 + HJ210	NJ2216 E.TVP2 + HJ216
	SL182206	SL182210	
Mineral oil	Aral Degol BG 220		
Polyglycol	Tribol 800/220		

ing axial load in dependency of the size and design of the bearing.

However, these details are only valid for the bearings of one manufacturer, and considerable safety margins are applied.

Testing Program

For this investigation (Ref. 10), five different designs of CRBs in three sizes are considered. For the evaluation of size effect, bearings with the bearing diameters $d = 30$, 50 and 80 mm are chosen. Rolling bearings are produced in different series. These series feature varying load ratings independent of the outer diameter, quantity of rolling elements and bearing width. Besides the bearing series 22, series 23 is examined. Bearings of the NJ design normally provide friction-optimized lip geometries. The lip is not orthographic to the raceway, but inclined with the lip angle ϕ. Furthermore, the lip can be crowned. The loose lip of a NUP design and an angle ring in contradiction do not feature a friction-optimized geometry. Their evaluation will demonstrate the influence of the lip geometry on the friction behavior of axial-loaded CRBs. Full-complement bearings employ the maximum possible number of rolling elements, whereby the radial load is shared by a greater number of contacts and thus leads to greater load rating. These bearings can be used as a supporting bearing like an NJ design because they also feature three lips.

The lubricant has a large influence on the friction behavior and, therefore, on the permissible thrust load of radial cylindrical roller bearings. Within this study a mineral oil and a poly glycol of the viscosity class ISO VG 220 are tested (Table 1).

In addition, all bearings feature normal clearance. The cage material is Polyamide 66. The friction torque measurements are performed at different combinations of speed and load. The gaps between the different speeds in the low-speed range are chosen smaller than at high speeds because the lubrication film thickness in the lip-roller contact grows with speed. With the rise in lubrication film thickness, the rate of mixed lubrication decreases and the hydrodynamic friction increases. The focus of this study is on the operation with mixed friction, for which reason the test speeds are chosen according to Table 2.

The tests at constant speeds are supplemented by run-ups; the test program is completed with run-in and wear experiments.

Friction Torque Measurements on Rolling Bearings

For the assessment of the behavior of combined-loaded CRBs—as well as of bearings in general—the global-measure friction torque is of decisive relevance. On one hand, resulting bearing temperature is directly dependent on the friction; on the other, conclusions regarding the lubrication condition can be drawn. In past years extensive measurements of bearing friction torques on different test rigs have been performed at Ruhr University-Bochum's Research Center for Mechanical Components and Power Transmission.

Lubenow (Ref. 4) and Koryciak (Ref. 8) used devices that allowed measurement of the friction torque on the outer ring of the test bearing. For this study a new test rig has been designed that allows measurement of the friction losses of multiple bearings with a torque measurement shaft. The detection of the friction torque is effected on the inner ring. Figure 2 shows that the result is affected by the measuring position due to the splashing of the rolling elements and the cage in the lubricant.

While the outer ring is standing still, the inner ring is driven with the necessary driving torque T_{drive}. The friction of the whole bearing has to be overcome and therefore the driving torque T_{drive} complies with the absolute value of the measured friction torque on the inner ring T_{IR}. Due to the splashing of the rolling elements and the cage, the drag torque T_{drag} results on the cage that is retained in the lubricant. The measured friction torque therefore is reduced by the amount of the drag torque. In the following the influence of the different measuring techniques on the results is examined. With the help of a modified test rig, the influence of the measuring position dependent on speed and oil level is investigated. The testing bearings are applied with the minimum radial load according to SKF (Ref. 6). While operating with minimum lubrication, the drag losses vanish; both measuring positions should show the same results. Dipping the shaft into the lubricants leads to additional drag losses that would influence the results; therefore the maximum oil level is limited to the inner ring of the test bear-

Table 2 Test speeds	
Inner ring speed, n, rpm	20, 50 100, 500, 1000, 3000, 5000

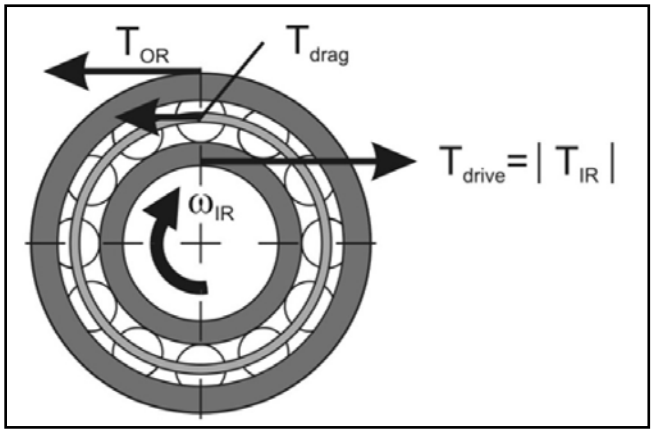

Figure 2 Measured friction torques of a bearing.

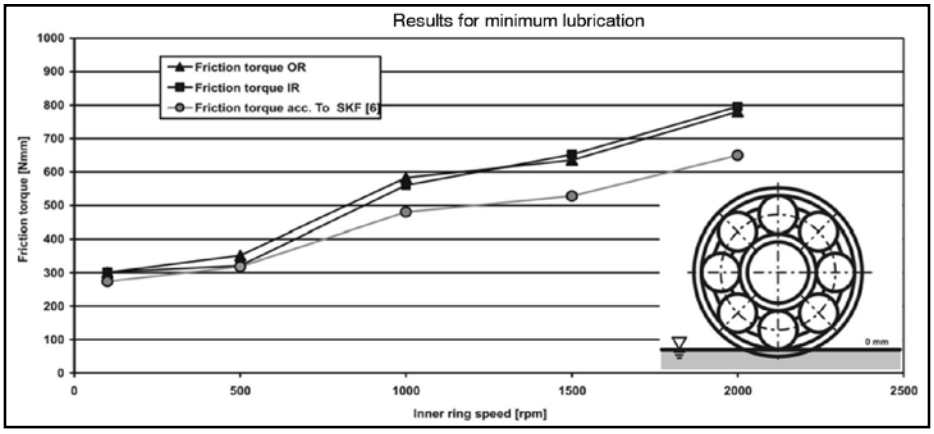

Figure 3 Friction torque at minimum lubrication.

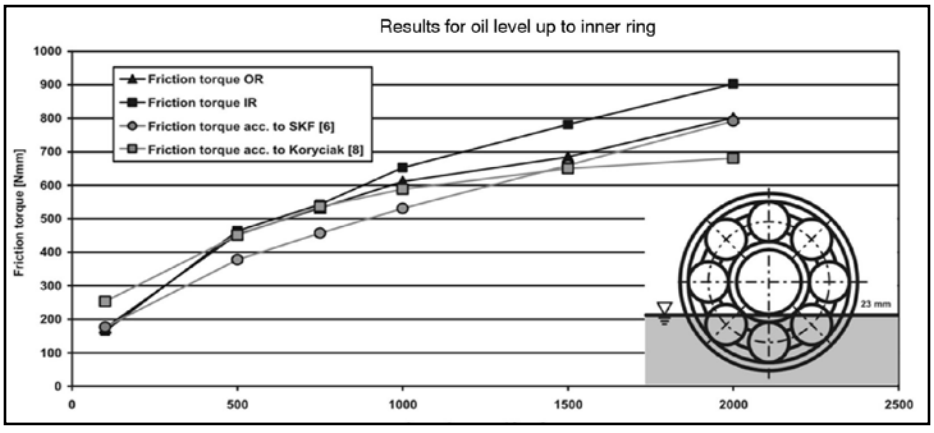

Figure 4 Friction torque at oil level "up to inner ring."

Table 3 Bearing geometry

	NJ2206	NJ2210	NJ2216
Bore diameter, *d*, mm	30	50	80
Outer diameter, *D*, mm	62	90	140
Bearing width, *B*, mm	20	23	33
Quantity of rolling elements, *n*	13	16	18
Rolling element diameter, d_w, mm	9	11	16
Rolling element width, l_w, mm	13	15	24
Static load rating, C_0, kN	50	88	245

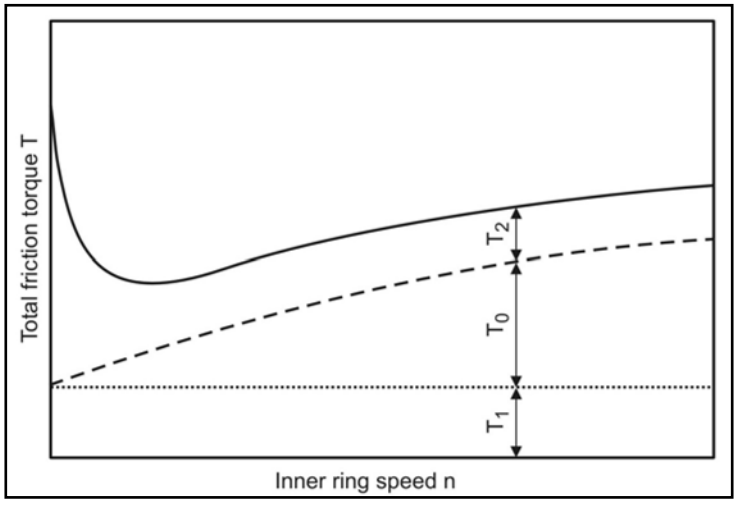

Figure 5 Distribution of friction torque dependent on inner ring speed.

ings. Between these extremes the levels "lowest-rolling-element-half-in-oil" and "lowest-rolling-element-in-oil" are defined (Fig. 3).

Figure 3 shows the total friction torque in dependence of the inner ring speed. The measuring results are compared with the calculation results according to SKF (Ref. 6). The deviation between the measured torques on the inner and outer ring are within the measurement precision. This proves the assumption that with the disappearance of the drag losses, the measuring position has no influence on the results. Furthermore, at low speeds the results follow the calculations according to SKF very well. At medium and high speeds, the calculated values are below the measured ones. Figure 4 summarizes the results for the maximum oil level. In addition to the SKF results, values calculated with the method of Koryciak (Ref. 8) are presented.

Figure 4 shows that with higher oil levels a rising difference of the measured torques can be observed from an inner ring speed of 1,000 rpm and higher. The measuring position on the outer ring also shows good correlation with the results documented by Koryciak (Ref. 8). Koryciak performed his examinations on test rigs which detect the friction torque on the outer rings of the test bearings. The conclusion is that with rising oil levels, differing friction torques are to be observed on inner and outer rings. Furthermore, the results show deviations in the range of 100 N-mm for the examined bearing. The measurements within this study were performed at considerably high radial and axial loads, which lead to much higher friction levels than observed in this presentation. In the range of high friction levels, greater deviations have to be taken into account, which easily can amount to several hundred N-mm. Considering this, the influence of the measuring position on the results can be ignored.

Results for Oil Level Up to Inner Ring

Influence of the bearing size. For the examination of the size effect, CRBs with 30, 50 and 80 mm bore diameter

are tested. Table 3 shows the relevant data of the NJ22 design.

Driven at constant speed, a rising bearing diameter induces a higher sum of velocities in the lip-roller contact. At a rising sum of velocities, the lubricant film thickness rises as well, meaning that the sum of velocities has great influence on the friction and wear behavior of the contact. At low speeds, the lip-roller contact is characterized by mixed lubrication, while at higher speeds the portion of hydrodynamic lubrication rises. For this reason there is a minimum at a certain speed range. Above the speed range with minimum friction, the drag losses grow larger (Fig. 5). The load-independent losses are represented by T_0, the radial load dependent friction torque is T_1, and the axial load-dependent friction torque is T_2.

Due to the differing sums of velocities and rising bearing diameters, the friction minimum is removed to lower speeds with rising bearing diameter. Concurrently, the axial load-dependent friction torque decreases, due to higher lubrication film thickness and attendant rising diameter, constant speed and load. The axial load-dependent friction torque is described as the product of the normal force in the lip-roller contact, a friction coefficient and the lever to the bearing axis. The lever grows with the bearing diameter, as does friction torque (Fig. 6).

Due to these described effects, the smallest bearing shows the highest axial load-dependent friction torque on the test rig. For the medium-size bearing, the lowest axial load-dependent friction torque can be observed, whereas the largest bearing has friction losses ranging exactly between the other ones (Fig. 7). To correctly interpret Figure 7, one must consider that the illustrated results are only valid for the axial load-dependent friction torque and that speed, temperatures and axial loads are held constant.

Influence of the Bearing Design

The examined bearing designs were introduced earlier in this presentation. Macroscopically, the different test bearings can be distinguished by the quantity and configuration of their lips.

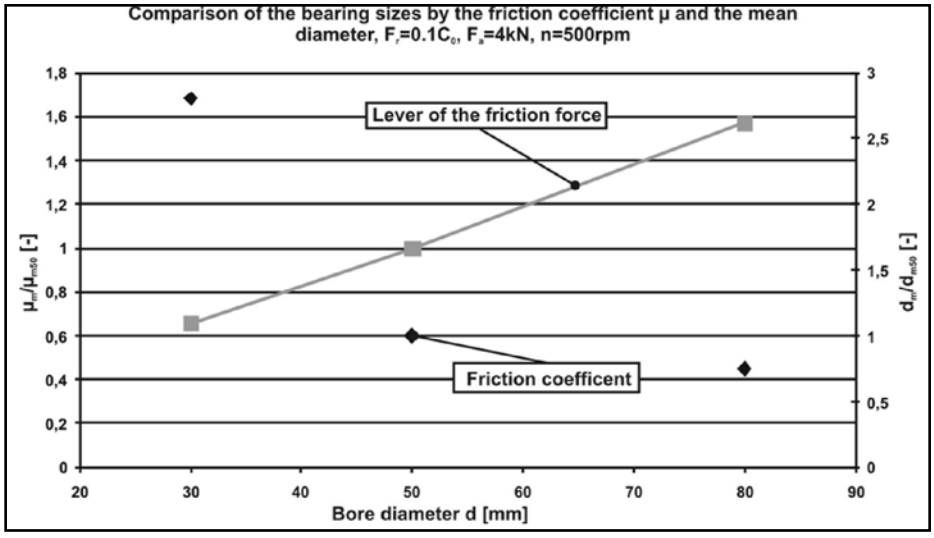

Figure 6 Friction coefficient and lever of the friction force on lip inner ring.

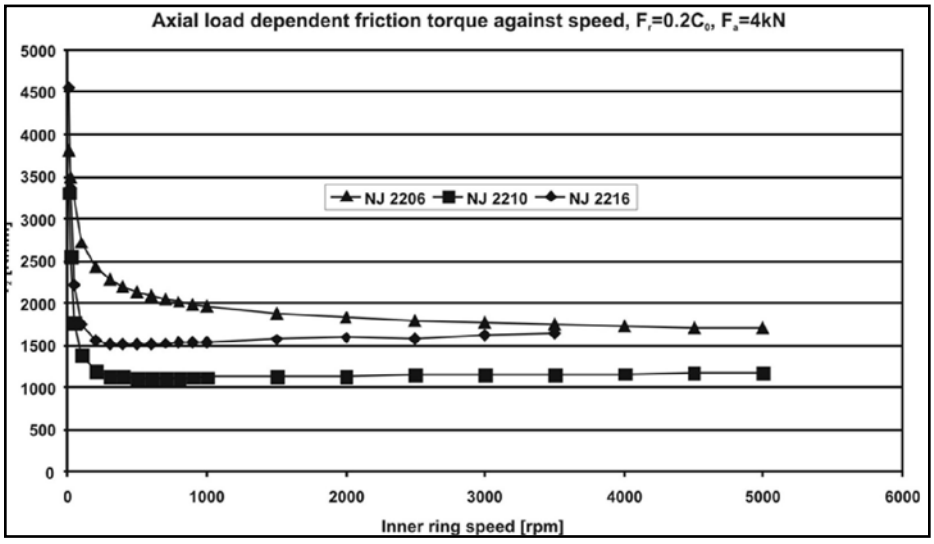

Figure 7 Axial load-dependent friction torque T_2 independent of speed and bearing size.

Additionally, full-complement CRBs and bearings of the "heavy" series NJ23 are investigated (Table 4).

As observed in Table 4, the full-complement bearing and the NJ2306 obviously differ from the remaining bearings. In this connection especially, the quantity of roller elements and their length are to be highlighted. Figure 8 shows measured total friction torques of the different bearing types determined in run-in tests. The test speed amounts to $n = 500$ rpm; the bearings are lubricated with mineral oil.

The bearing loads were chosen according to their static load rating C_0, for which reason the total friction torque of the variants NJ2306 and SL182206 exceeds that of the remaining bearing variants. In the matter of the full-complement bearing, the roller elements contact; this contact induces higher frictional losses due to their rotation in opposing directions.

Figure 8 shows a minor run-in of the NJ2206 during the first 50 operating hours. The reduction of friction amounts to approximately 500 N-mm and is considerably lower than observed in earlier examinations. This observation can be explained by lower roughness before the start of the test. As already mentioned, the loose lip and the angle ring do not feature an optimized lip geometry.

What's more, the roughness is higher than that of the NJ bearing lip. For these reasons these variants show a more distinct run-in effect. The combination of a NJ2206 and an angle ring reaches a similar friction level as a thrust-loaded NJ2206 without an angle ring.

The NUP bearing does not reach the full run-in state (Fig. 8). Tests with the larger bearing NUP2210 show that a complete run-in bearing with a loose lip can have friction torque similar to an NJ bearing. And like the NJ2206, the NJ2306 does not show a run-in effect. The full-complement CRB, despite its lower roughness, shows a significant run-in effect. This is not to be traced back to a run-in process in the lip-roller contact, but rather to a run-in process in the contact between the rolling elements amongst each other. To summarize, the axial load-dependent friction torque of all considered bearing designs is on the same level as if they were completely run-in.

Table 4 Geometry of tested bearings with 30 mm bore diameter

	NJ2206	NUP2206	NJ2206 +HJ206	NJ2306	SL182206
Bore diameter, d, mm	30				
Outer diameter, D, mm	62			72	62
Bearing width, B, mm	20			27	20
Number of rolling elements, n	13			12	16
Rolling element diameter, d_w, mm	9			11	9
Rolling element length, l_w, mm	13			18	14
Number of lips on the inner ring	1	2	2	1	2
Number of lips on the outer ring	2				1

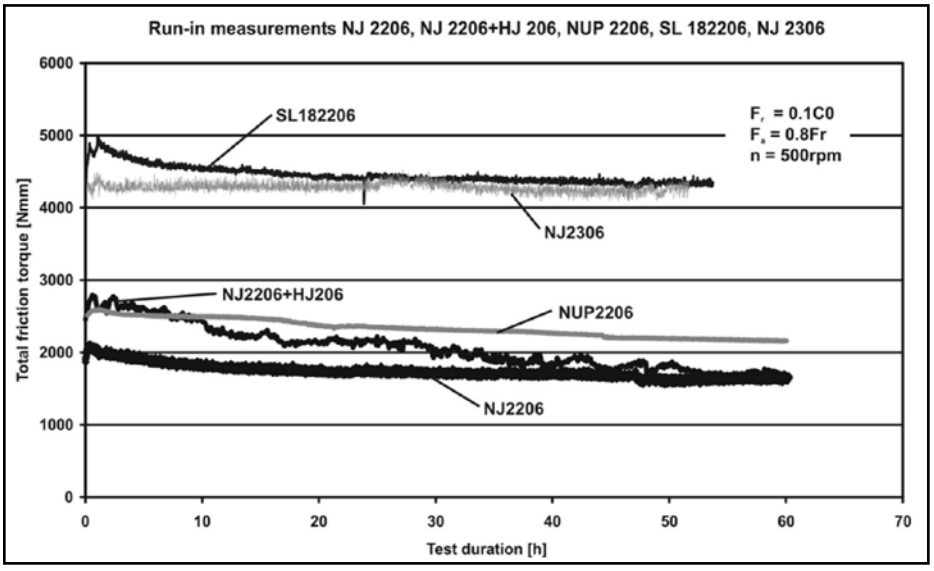

Figure 8 Run-in measurements.

Approximation Equations

In the scope of this study, approximation equations are developed that allow the calculation of the axial load-dependent friction torque of CRBs. Only common sense dimensions are used for these equations; the microgeometry of the bearings is omitted. Figure 9 shows a comparison of the results from the approximation equations and those from the simulation model (Ref. 9).

The left part of Figure 9 shows the results from the approximation equations, whereas the results from the simulation model are illustrated at the right. The calculations are based on an NJ2206 bearing that is operated in the experimentally investigated parameter range. Figure 9 displays good correlation among the simulations from the simulation model with those from the approximation equations. Only in the range of high loads at low speeds do the approximation equations lead to higher values than calculated by the simulation model.

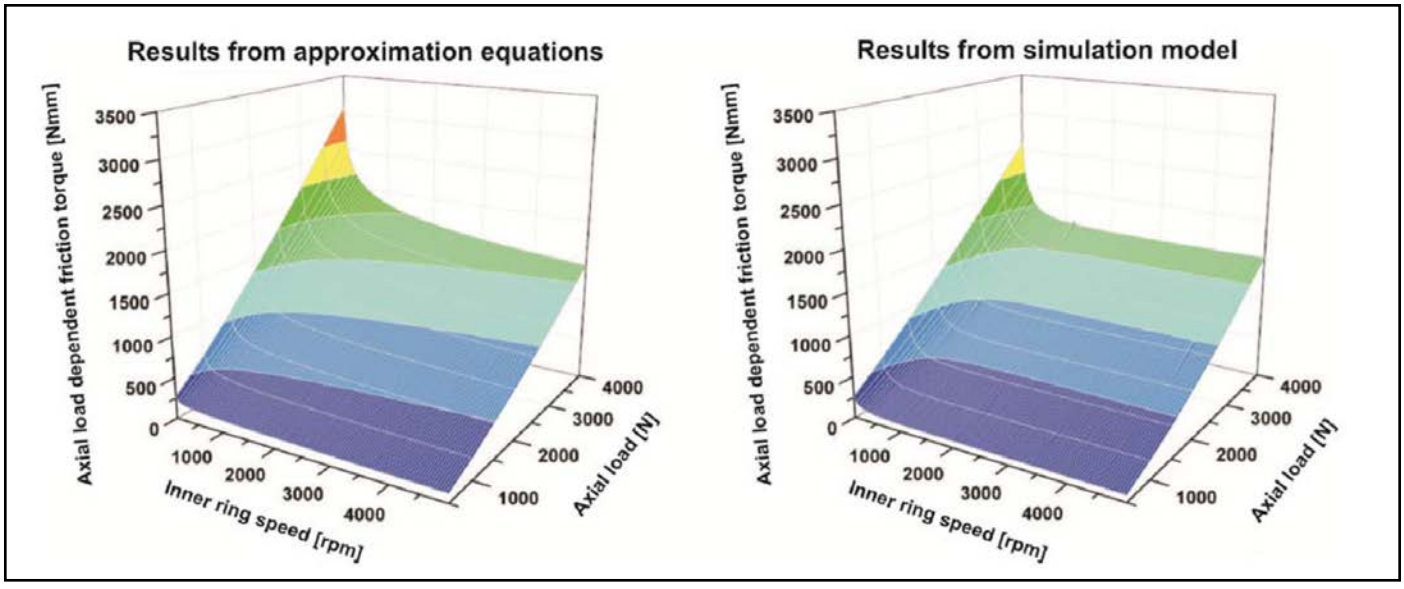

Figure 9 Results from the approximation equations vs. results from the simulation model (Ref. 9).

Summary

The aim of this study is the examination of the axial load-carrying capacity and of the axial load-dependent friction torque of cylindrical roller bearings. Extensive test runs are performed with five different bearing designs and three different sizes. The decisive measure is the bearings' friction torque. Besides size and design of the bearings, the operation parameters of speed, loading and lubricant are varied. The tests included comprehensive measurement of equilibrium, run-ups, running-in and wear experiments. A simulation model that has been developed at RUB allows the calculation of the axial load-dependent friction torque, load distribution, Hertzian stresses and lubrication film thicknesses (Refs, 4 and 9).

The results achieved within this study allow for the validation of this simulation model. This study is comprised of the development of approximation equations that allow the calculation of the axial load-dependent friction torque with parameters that are known to the designer. The results are the basis for the determination of the permissible axial load with a heat balance of the bearing. **PTE**

References

1. FAG. Wälzlager auf denWegen des Technischen Fortschritts, Verlag R. Oldenbourg GmbH, München, 1984.
2. FAG. Hauptkatalog WL41 520/3 DB, 1999.
3. Bartels, T. Bordreibung von Zylinderrollenlagern – Iteraturrecherche, Forschungsthema T609, Forschungsvereinigung Antriebstechnik e.V., Heft 420, 1994.
4. Lubenow, K. "Axialtragfähigkeit und Bordreibung von Zylinderrollenlagern," Dissertation und Schriftenreihe des Instituts für Konstruktionstechnik, Heft 02.2, Ruhr-Universität Bochum, 2002.
5. Schaeffler KG. Wälzlager HR1, 2006.
6. SKF. Hauptkatalog 5000 G, 2004.
7. Brändlein, J., P. Eschmann, L. Hasbargen and K. Weigand. Die Wälzlagerpraxis, Handbuch für die Berechnung und Gestaltung von Lagerungen, 3. Auflage, Vereinte Fachverlage GmbH, Mainz, 2002.
8. Koryciak, J. "Einfluss der Ölmenge auf das Reibmoment von Wälzlagernmit Linienberührung," Dissertation und Schriftenreihe des Instituts für Konstruktionstechnik, Heft 07.1, Ruhr-Universität Bochum, 2007.
9. Koch, O. "Dreidimensionale Simulation von Kombiniert Belasteten Zylinderrollenlagern," Dissertation und Schriftenreihe des Instituts für Konstruktionstechnik, Heft 08.1, Ruhr-Universität Bochum, 2008.
10. Söndgen, S. "Verlustleistung und Tragfähigkeit belasteter Borde von Zylinderrollenlagern," Dissertation und Schriftenreihe des Instituts für Konstruktionstechnik, Heft 09.5, Ruhr-Universität Bochum, 2009.

Prof. i.R. Dr.-Ing. Wolfgang Predki was the head of the chair of Mechanical Components and Power Transmission, located at the Ruhr-University Bochum, Germany, until his retirement in 2012.

Dr.-Ing. Simon Söndgen was a staff member at the chair of Mechanical Components and Power Transmission, located at the Ruhr-University Bochum, Germany from 2005–2009. He earned his engineering doctorate there in 2009 based on his investigation of the power loss and axial load-carrying capacity of radial cylindrical roller bearings. He has worked since 2011 in the engineering and development department of Zollern Getriebetechnik Dorsten GmbH & Co. KG, focusing on main gearboxes for wind turbines and large gearboxes for industrial applications. In February of this year he was named head of product management industry applications.